# Effect of Block Copolymer Adsorption on Thin Film Dewetting Kinetics

**Robert Oslanec,† Ana Claudia Costa, and Russell J. Composto***

*Department of Materials Science & Engineering and Laboratory for Research on the Structure of Matter, The University of Pennsylvania, Philadelphia, Pennsylvania 19104-6272*

**Petr Vlcek**

*Institute of Macromolecular Chemistry, Academy of Sciences of the Czech Republic, Heyrovsky Square 2, 162 06 Prague 6, Czech Republic*

*Received November 16, 1999*

ABSTRACT: The stability of polystyrene (PS) films on silicon oxide is improved by blending with poly(styrene-*block*-methyl methacrylate) (PS-*b*-PMMA) having a short, adsorbing MMA block and long, dangling PS block (degree of polymerization $N$). Relative to PS (degree of polymerization $P$), hole growth velocity decreases by 5 and 17 times upon adding 0.05 volume fraction of PS-*b*-PMMA ($\phi$) for $N \sim P$ and $N \sim 4P$, respectively. In contrast to PS, holes approach a constant value and do not coalesce. The $N \sim 4P$ system provides better stabilization because of its broader interfacial width. For $N \sim P$, hole velocity decreases as $\phi$ increases and then becomes constant for $\phi > 0.03$. Relative to blends, holes grow faster in bilayers and eventually coalesce. AFM analysis shows that the PS hole floor is smooth whereas the blend floor contains patches. The film stabilizing effect of block copolymers can be attributed to a decrease in capillary driving force, entanglements at the matrix/copolymer interface, and brush grafting density.

## 1. Introduction

Thin polymer films and their stability are important to many technological areas, including microelectronics, coatings, lubricants, and adhesives. A contiguous thin film of a liquid or polymer on a substrate will tend to minimize its free energy by exposing the lower surface energy material to the environment. If the surface energy of the coating, $\gamma_c$, is lower than that of the underlying substrate, $\gamma_s$, the film is stable. On the other hand, if $\gamma_c$ is larger than $\gamma_s$, the system can reduce its free energy by creating holes in the coating, thus exposing the substrate to air. This process is called *dewetting*. The stability of the coating can be expressed in terms of a *spreading coefficient*, $S$,

$$S = \gamma_s - (\gamma_c + \gamma_{cs}) \tag{1}$$

where $\gamma_{cs}$ is the coating/substrate interfacial energy. If $S$ is positive, the coating will wet the substrate and the film will be stable. If $S$ is negative, however, the coating will dewet the substrate and the contact angle for the coating material on the substrate will be greater than zero. In addition to the surface and interfacial energies, thin film dewetting will depend on other contributions, in particular the film thickness. For relatively thick films (>1000 Å) the balance between interfacial and hydrostatic or gravitational forces will dominate the van der Waals forces and determine film stability.[1] Therefore, films thicker than ca. 1000 Å but thinner than ca. 1 $\mu$m will be metastable even when $S$ is negative.[1,2] In films thinner than ca. 1000 Å, attractive van der Waals forces dominate, causing the thin film to rupture spontaneously.[1,3] Khanna and Sharma[4] investigated the effect of van der Waals forces on thin film stability.

The theory of thin film dewetting on solid substrates has received considerable attention.[1,2,5−8] Here, we will focus on relevant experiments. Reiter[9,10] and Sharma et al.[11] used optical microscopy to investigate the dewetting of thin (<1000 Å) polystyrene (PS) films on silicon substrates. Upon annealing above its glass transition temperature, the PS films formed holes with rims. Later, the rims between neighboring holes impinged and formed a cellular pattern which then broke up into PS droplets. Similar behavior was observed by Shull and Karis[12] for poly(ethylene-*co*-propylene) (PEP) deposited on glassy PS or poly(methyl methacrylate) (PMMA) substrates. The dewetting of PEP from silicon was also studied by Zhao et al.[13] using X-ray reflectivity and atomic force microscopy. These authors found that films thinner than the PEP radius of gyration dewetted the substrate and formed irregularly shaped droplets.

Polymer thin film stability can be improved by increasing the chemical and physical interaction between the coating and substrate. For example, Feng et al.[14] used metal counterions ($Li^+$, $Zn^{2+}$) to stabilize thin films of sulfonated polystyrene on silicon oxide. The ionomer complexation and long-range electrostatic interactions were responsible for retarding dewetting. A combined chemical and physical approach uses polymer adhesion promoters, which anchor one side of the chain to the substrate and entangle the other side with matrix chains to form a *polymer brush*. Anchoring polymer chains to the solid substrate by one end may induce steric constraints, resulting in stretching the polymer molecules.[15] The stretching, in turn, results in entropic repulsion of nongrafted molecules. Therefore, a distinct interface with nonzero interfacial tension between the brush and the coating polymer is formed. When the matrix chain length, $P$, is considerably larger than that of the grafted chain, $N$, the nongrafted chains have a finite penetration into the brush. At very high graft densities, these free chains will not wet its own brush, leading to *autophobic* behavior described first by Leibler et al.[16] and later in more detail by Shull.[17,18] Autophobic behavior was in fact observed several decades ago by

† Current address: BHP Institute for Steel Processing and Products, University of Wollongong, Wollongong, NSW 2522 Australia.

10.1021/ma9919312 CCC: $19.00 
Published on Web 07/08/2000

Hare and Zisman,[19] who observed that polar molecules (e.g., amines, alcohols) did not spread on their own monolayers.

For polymer films, autophobic behavior was first observed by Leibler et al.,[16] who observed that small droplets of PS did not wet a dense PS brush formed by PS-*b*-PMMA lamellae. In similar experiments, upon depositing PS films on poly(vinylpyridine)-*b*-PS lamellae, Liu et al.[20] observed that only PS films with high $P$ would dewet, in agreement with theory.[16] By varying the graft density of anchored PS chains, autophobic behavior was investigated systematically by Reiter et al.[21,22] and Henn et al.[23] Recently, Kerle et al.[24] investigated the wetting properties of thin films on top of an identical cross-linked network. Whereas the film wets the network at low cross-linking densities, partial wetting was observed at intermediate cross-linking, suggesting that the network is similar to a high-density brush.

Grafted homopolymers or adsorbed block copolymers at the polymer/substrate interface do not always result in autophobic behavior. Theoretical studies by Martin et al.,[25] Brochard-Wyart et al.,[26] and Long et al.[27] showed that an adsorbed layer of chemically identical polymer had a dramatic effect on polymer film dewetting. The dewetting dynamics can be slowed by viscoelastic breaking[27] or by entanglements between the adsorbed polymers and the matrix polymers.[26] The adsorbing species could be either a low grafting density brush or a polydisperse brush, where the long chains act as connectors and effectively anchor the film to the substrate. The adsorbed polymer also decreased the spreading coefficient (eq 1) and therefore the driving force for dewetting.

Yerushalmi-Rozen and co-workers[28−30] were the first to show that the dewetting of thin oligomer PS film was significantly slowed by grafting a PS brush with low grafting density to the substrate and, at the same time, adding high molar mass PS chains to the film. In these experiments, the high molar mass PS acted as a connector, which easily penetrated the brush and entangled with the oligomer PS molecules. Film stability could also improve because the addition of long PS chains can increase the film viscosity. Reiter and coworkers[21,22] observed that the dewetting rate increased as the grafting density of a PS brush increased. In addition, for a PS film ($P = 413$), the role of connectors, long end-functionalized chains ($N = 418$ and 1215) mixed with shorter brush chains ($N = 89$), was investigated.[22] Bimodal brushes having a low amount of long connector chains significantly decreased the dewetting dynamics and, above a threshold grafting density, even stopped dewetting. The threshold grafting density was about $10.5 \times 10^{-3}$ chains/nm$^2$ for the shorter connectors, whereas only about $^1/_3$ of this amount was needed for longer connectors. Film stabilization was attributed to the energy cost associated with disentanglement of connector chains from the matrix chains by chain pullout. Recently, Reiter et al.[31] investigated poly(dimethysiloxane) (PDMS) homopolymer films on bimodal PDMS brushes of long connectors and short chains. Using the same bimodal brush, the PDMS film thickness was increased to demonstrate that very weak van der Waals interactions can influence film stability. Yuan et al.[32] recently investigated the influence of surface-active fluorocarbon-terminated PS (PS−F) additives on the dewetting dynamics of thin PS films deposited onto PMMA substrates. For these bilayer systems, the PS−F additive was found to slow down and, in certain cases, stop dewetting.

In the previous studies, a polymer brush was formed by end-functionalized homopolymers or by block copolymer lamella. Until now, diblock copolymers with an adsorbing anchor and a dangling, nonadsorbing tail received little attention as thin film stabilizers. Yerushalmi-Rozen and Klein[30] used block copolymers of deuterated PS and poly(ethylene oxide) (dPS-*b*-PEO) containing a short PEO block ($N = 341$) and a long dPS block ($N = 4330$). The PEO block adsorbs strongly to silicon oxide, whereas dPS, the nonadsorbing block, forms the brush. For both an end-functionalized PS and dPS-*b*-PEO, two different methods of sample preparation were used. In the first, the polymer brush was prepared on the substrate, and then a PS film was placed over the brush. This "bilayer" approach was also used in the previously mentioned studies. In the second route, 4.5% of the additive was blended with the matrix polymer and deposited on the substrate to form a homogeneous film. A significant difference between approaches is that in the latter case polymer adsorption occurs simultaneously with hole formation. The authors state that both blends and bilayers yielded equivalent results. Namely, thin film stabilization was achieved for both end-functionalized PS and dPS-*b*-PEO brushes when $N$ was greater than $P$.

In this paper, we study the dewetting dynamics of thin films of polystyrene (PS) having a degree of polymerization $P$ deposited on oxide-covered silicon wafers ($SiO_x$) using optical and atomic force microscopies. Upon adding 0.05 volume fraction of poly(styrene-*block*-methyl-methacrylate) (PS-*b*-PMMA) to the film, hole growth velocity decreases relative to the pure PS film, and the holes eventually stop growing before they can coalesce. The hole growth for PS-*b*-PMMA additives having PS block lengths of $N \sim P$ and $N \sim 4P$ is investigated to study the effect of interfacial width on dewetting behavior. In agreement with theoretical predictions,[25−27] the $N \sim 4P$ system is the most effective stabilizer due to its greater matrix chain penetration into the brush. For the $N \sim P$ system, the hole velocity decreases as the copolymer volume fraction $\phi$ increases and then becomes constant for $\phi$ larger than 0.03. The PS-*b*-PMMA copolymer is also deposited directly on the oxide substrate to compare bilayer sample preparation with blending. Specifically, in the bilayer case, hole growth is faster than in the blend case. Furthermore, holes coalesce and eventually the film breaks into droplets, consistent with autophobic behavior. Relative to the PS film, AFM analysis of the hole floor of the blend reveals a smaller contact angle, an irregular-shaped rim, and residual patches of polymer inside the hole.

## 2. Experiment

The characteristics of the matrix polymer and diblock copolymers are given in Table 1. The PS-*b*-PMMA[33] is asymmetric having a short MMA block, which adsorbs to $SiO_x$, and a long PS block with chain length $N$, which prefers to mix with the matrix chains.[34] The PS matrix polymer was purchased from Pressure Chemical. To probe the influence of brush penetration, we have chosen one PS-*b*-PMMA with $N \sim P$ and the other with $N \sim 4P$.

The substrates were prepared by etching a silicon wafer for 3 min in a hydrofluoric acid:water solution (1:7) to remove the native oxide. The substrate was then placed in an ultraviolet

**Table 1. Polymer Characteristics**[a]

| polymer ID | no. of segments | MMA content [mol %] | Pd index | mol wt [g/mol] |
|---|---|---|---|---|
| PS-*b*-PMMA ($N \sim P$) | $N = 301$; MMA = 28 | 8.6 | 1.55 | 34 000 |
| PS-*b*-PMMA ($N \sim 4P$) | $N = 1126$; MMA = 34 | 2.9 | 1.34 | 120 600 |
| PS | $P = 288$ | | 1.03 | 30 000 |

[a] $N$ = number of styrene segments in copolymer. MMA = number of methyl methacrylate segments in copolymer. $P$ = number of styrene segments in matrix polymer.

ozone cleaner for 10 min to produce a clean ca. 20 Å thick $SiO_x$ film, as measured by ellipsometry. Two different sample geometries were used. In the first case, polymer blends were prepared by spin-coating a toluene solution of a blend of PS-*b*-PMMA and PS on the substrate. Film thickness as measured by ellipsometry for the blend samples ranged from 770 to 820 Å. To study the effect of $N$, the volume fraction of PS-*b*-PMMA ($\phi$) in the as-cast films was fixed at $\phi = 0.05$. To investigate the effect of $\phi$, $\phi$ was varied from 0.01 to 0.1 for the $N \sim P$ system. The samples were dried in a vacuum oven at 80 °C for 24 h. In the second case, bilayer samples were prepared by first spin-coating a block copolymer film of thickness 75 Å directly on the substrate. The copolymer layer was first dried in a vacuum oven at 80 °C for 24 h and then annealed at 175 °C for 24 h. Then, a PS film was prepared on a glass substrate, dried, floated on water, and picked up with the block copolymer/silicon oxide sample. To match the blend composition of $\phi = 0.10$, the thickness of the top layer was chosen such that the total bilayer thickness was about 720 Å. The bilayer sample was then dried in a vacuum oven at 80 °C for 24 h.

The holes in the film were initiated by preannealing samples in a vacuum oven at 175 °C for 5 min. After mapping the hole distribution under an optical microscope, samples were placed on a Mettler FP90 hot-stage preheated to 175 °C, where the dewetting kinetics were measured under nitrogen flow at 175 °C. The length scale of the images was calibrated by recording an image of the microscope calibration ruler with 10 $\mu$m line spacing. Hole growth was measured until holes touched each other or hole diameter appeared constant.

Using a Digital Instruments NanoScope III atomic force microscope (AFM), the hole floor morphology and rim were imaged for a PS film and a blend of PS and PS-*b*-PMMA ($\phi = 0.05$, $N \sim P$). To compare holes of similar size, the PS and blend films were annealed for 30 and 600 min, respectively, to create holes of ca. 15 $\mu$m. Samples were then quenched to room temperature, below the PS glass transition temperature, and viewed by AFM in the glassy state. The AFM images were recorded in air at room temperature using a Si tip in tapping mode. The scanned area was 6 $\mu$m × 6 $\mu$m using a scan rate of 1 Hz. The reproducibility and sample damage were checked by scanning from left to right and then from right to left. No differences in topography were observed for these images.

## 3. Results

The adsorption of dPS-*b*-MMA to silicon oxide from a matrix polymer has been studied as a function of matrix degree of polymerization, $P$,[35,36] and matrix composition.[37] As $P$ increases, the interfacial excess, $z^*$, increases rapidly and then becomes constant for $P$ larger than $2N$, where $N$ is the dPS block length. The interfacial width representing the overlap between the dangling dPS block and the matrix chains was found to narrow with increasing $P$ and eventually reached a constant value for $P > 2N$. These measurements were explained in terms of the entropic repulsion between the matrix chains and the brush. One objective of the present paper is to test whether block copolymer adsorption, with known adsorption characteristics, can retard or prevent thin films deposited on silicon oxide from dewetting. Furthermore, we will probe the effect of interfacial overlap on dewetting by studying two PS: PS-*b*-MMA blends having $N \sim P$ and $N \sim 4P$, which represent relatively dry and wet brushes, respectively.

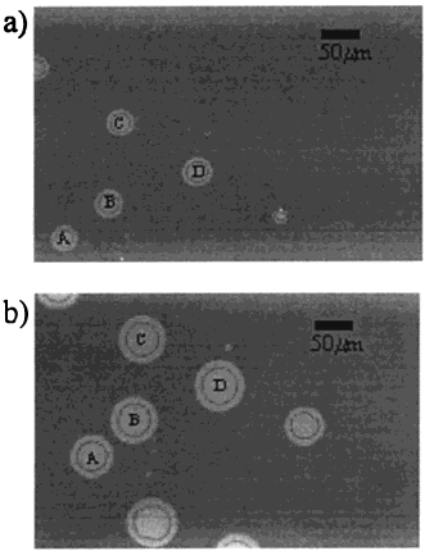


**Figure 1.** Optical micrographs showing holes (light) in a PS film (822 Å) annealed at 175 °C for (a) 12 min and (b) 50 min. The hole rim is represented by the bright outer ring. The thin dark ring separates the rim from the hole floor and therefore represents the hole diameter. AFM analysis of the hole supports these observations. Holes nucleated at the same time are denoted as A, B, C, and D.

To optimize the additive amount, hole growth will be studied as a function of PS-*b*-MMA concentration. To provide insight into the dewetting mechanism, the morphology of the hole floor will be imaged using AFM.

**3.1. Block Copolymer Additives.** Dewetting of thin PS films has been well-documented.[9−11] Figure 1 shows hole growth in PS ($P = 288$) films (822 Å) at 175 °C after (a) 12 min and (b) 50 min of annealing. With one exception, the holes shown in Figure 1a,b nucleate at the same time. For example, holes denoted as A, B, C, and D all grow at similar rates. The material from the hole goes into the circular rim, the bright outer ring. The hole diameter is defined by the inside rim wall, shown as a thin dark ring in Figure 1. This definition is supported by AFM, FE-SEM, and OM analysis from a previous study.[38] Figure 2 shows the hole diameter, $D$, plotted as a function of annealing time, $t$, for a PS film (open circles). Initially, $D$ increases linearly with time and then follows a $t^{2/3}$ power law, in agreement with predictions by Brochard-Wyart et al.[8] The initial hole growth velocity, $v_i$, is 0.69 $\mu$m/min. After 125 min (crossed open circle), the holes impinge upon one another, and the rims form an interconnected network.

Samples were prepared by blending PS with PS-*b*-MMA having a short PS block, $N \sim P$, or a long block, $N \sim 4P$. Because the MMA block lengths are similar, ca. 30, the MMA mole fractions are 0.09 and 0.03, respectively (cf. Table 1). Upon adding 0.05 volume fraction of PS-*b*-MMA, Figure 2 shows that copolymers of the short (solid circles) and long (stars) PS blocks dramatically reduce the rate of hole growth and prevent hole coalescence within the experimental time frame.

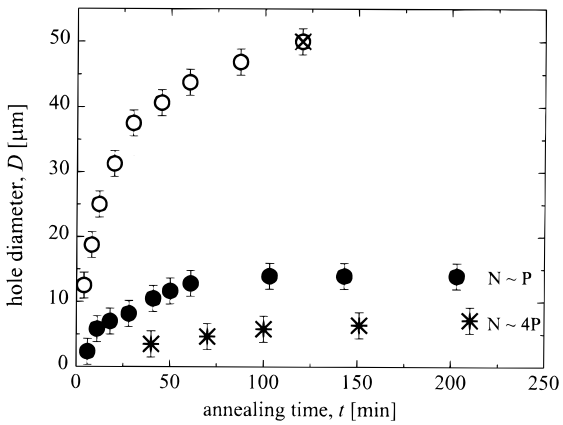


**Figure 2.** Hole diameter, $D$, as a function of annealing time, $t$, for pure PS (822 Å) (open circles), PS blended with PS-*b*-PMMA ($N \sim P$) (810 Å) (solid circles), and PS with PS-*b*-PMMA ($N \sim 4P$) (823 Å) (stars). For both blends, the PS-*b*-PMMA volume fraction is 0.05. The error bars (±2 $\mu$m) are estimated from the calibration ruler with line spacing 10 $\mu$m. For the PS film, the crossed circle denotes that holes touch.

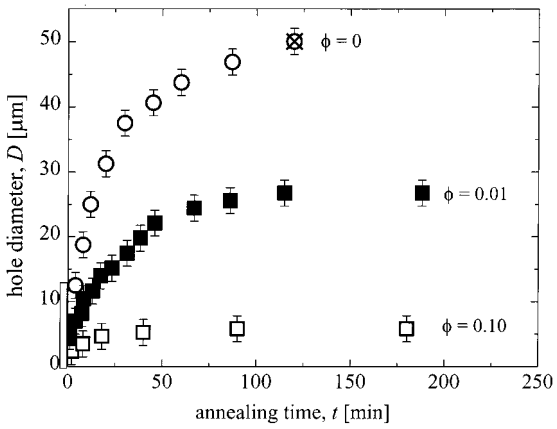


**Figure 3.** Hole diameter as a function of annealing time for pure PS with $\phi = 0$ (822 Å) (open circles), PS:PS-*b*-PMMA with $\phi = 0.01$ (778 Å) (solid squares), and PS:PS-*b*-PMMA with $\phi = 0.10$ (770 Å) (open squares). For both blends, the PS-*b*-PMMA has $N \sim P$. The error bars (±2 $\mu$m) are estimated from the calibration ruler. For the PS film, the crossed circle denotes hole impingement.

Note that in one system the additive and matrix have similar chain length ($N \sim P$), and therefore slowing down is not due to an increase in viscosity. Upon adding PS-*b*-MMA with short and long PS blocks, $v_i$ decreases by a factor of 5 and 17, respectively. After 100 min, the hole diameter approaches 14 and 7 $\mu$m for the short and long PS-*b*-MMA additives, respectively. Whereas $D$ approaches a constant value for the blend with $N \sim P$, $D$ continues to slowly increase after 100 min for $N \sim 4P$. For comparison, the holes in the pure PS film are ca. 50 $\mu$m after 100 min. Qualitatively, the number of holes per unit area was greatest for the pure PS and lowest for the PS blended with the PS-*b*-MMA having the longer PS block. The smaller number of holes in the blend samples further delays hole impingement. Samples annealed up to 24 h showed no measurable increase in $D$.

Figure 2 shows that the hole velocity is slower and the hole diameter is smaller for the blend with the long PS block in qualitative agreement with theoretical predictions[25−27] and experiments with end-functionalized brushes.[21] For dPS-*b*-PMMA adsorption at the PS/$SiO_x$ interface,[36] the matrix chain penetration into the dangling dPS block region decreases as $P$ increases and reaches a constant value near $P = 2N$. Dewetting experiments were performed at constant $P$ where the block copolymer additives corresponded to either a short PS block, $N \sim P$, or a long block, $N \sim 4P$. These results suggest that frictional drag at the interface between the adsorbed PS-*b*-MMA layer and the matrix can greatly retard hole growth.

**3.2. Bulk Volume Fraction of Block Copolymer Additive.** The dewetting kinetics of PS films were studied as a function of the bulk volume fraction, $\phi$, of PS-*b*-MMA with the short dangling block ($N \sim P$). Figure 3 shows the hole diameter as a function of annealing time for $\phi = 0$ (open circles), $\phi = 0.01$ (solid squares), and $\phi = 0.10$ (open squares). For clarity, the hole growth data for $\phi$ between 0.01 and 0.10 are absent. The hole growth for the pure PS film was presented in Figure 2 and previously discussed. Figure 3 indicates that the addition of only 1% PS-*b*-MMA to the PS film causes an appreciable slowing down of the hole growth rate. Furthermore, the holes approach a constant diameter of 26 $\mu$m after ca. 100 min. By increasing $\phi$ to 0.10, the hole growth rate is even slower, and the hole diameter approaches 6 $\mu$m, after only ca. 25 min.

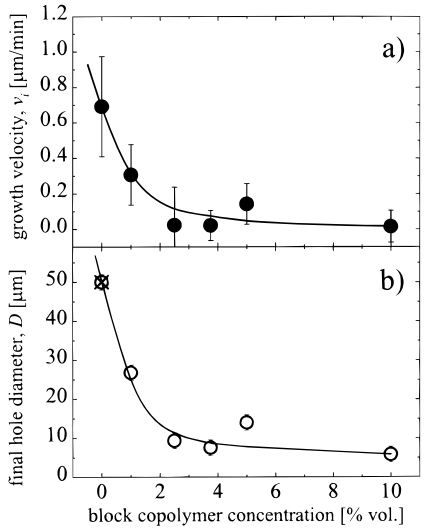


**Figure 4.** (a) Initial hole growth velocity, $v_i$ (solid circles), and (b) final hole diameter, $D$ (open circles), for PS blended with PS-*b*-PMMA ($N \sim P$). The error bars for $v_i$ were obtained from the standard deviation of linear fits of $D$ vs $t$ at low $t$. The error bars (±2 $\mu$m) for $D$ were estimated from the calibration ruler. For reference, the $D$ for PS prior to impingement is included and denoted by a crossed circle. The lines are guides to the eye only.

The initial growth velocity and the final hole size are plotted as a function of copolymer concentration in Figure 4. Figure 4a shows that the initial hole growth velocity decreases rapidly as $\phi$ increases from 0 to 0.03 and then becomes relatively constant. Similar behavior can be observed for the final hole diameter (cf. Figure 4b), which decreases rapidly as $\phi$ increases from 0 to 0.03 and then becomes relatively constant. These results demonstrate that low concentrations of block copolymer additives can improve thin film stability. These results are in qualitative agreement with observations by Jerushalmi-Rozen et al.[28−30] and Reiter et al.,[21,22] who found that film stabilization could be achieved at very low grafting densities.

**3.3. Blending versus Bilayer.** As already mentioned, the study of adhesion promoters typically in-

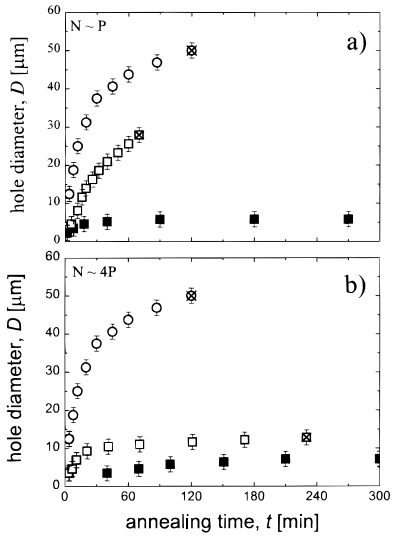


**Figure 5.** Hole diameter as a function of annealing time for the pure PS film (open circles), a bilayer of PS over PS-*b*-PMMA (open squares), and a blend of PS and PS-*b*-PMMA (solid squares). The overall PS-*b*-PMMA volume fraction is 0.10 for the blend and bilayer. In (a) and (b), the PS-*b*-PMMA corresponds to $N \sim P$ and $N \sim 4P$, respectively. The error bars ($\pm 2$ $\mu$m) were estimated from the calibration ruler. Note that the holes in the PS film and bilayers continue to grow until they touch each other (crossed symbols) whereas the holes in the blend samples approach a constant value.

volves a direct application of the promoter to a substrate followed by the application of a thicker matrix film over this thin layer. Figure 5 shows the hole diameter as a function of annealing time for PS, a PS:PS-*b*-MMA blend, and a PS/PS-*b*-MMA bilayer for (a) $N \sim P$ and (b) $N \sim 4P$. For the bilayer samples, the thicknesses of the copolymer and PS layers were chosen such that the overall $\phi$ is 0.10, which is the same value as the blend samples.

For both cases, Figure 5 shows that the initial rates of hole growth for bilayer samples (open squares) are faster than for the blends (solid squares). In addition, for both bilayers, holes grew until they impinged on each other, as denoted by the cross inside the open square. In these samples, the films eventually broke up into isolated droplets, similar to the pure PS film. These results demonstrate that a block copolymer layer deposited directly on the substrate is less effective than blends at stabilizing thin polymer films. Because the PS-*b*-MMA film is approximately a monolayer thick, the PS film on top of this dense adsorbed layer exhibits the autophobic behavior previously observed by Leibler et al.,[16] Reiter et al.,[21,22] and Henn et al.[23] Comparison of parts a and b of Figure 5 shows that bilayer samples with the long PS block ($N \sim 4P$) are more effective at slowing down hole growth than the bilayers containing the short PS block ($N \sim P$). In the former case (Figure 5b), the holes grew very slowly and reached a diameter of 12 $\mu$m before impinging upon each other after 230 min. Although the hole density was smaller in the latter case (Figure 5a), the holes impinged after only 70 min at a diameter of 28 $\mu$m because of their rapid growth.

For blends with 10% copolymer additive, film stabilization was observed for both $N \sim P$ and $N \sim 4P$ as shown in parts a and b of Figure 5, respectively. For $N \sim P$, the holes stopped growing at 6 $\mu$m after about 90 min, whereas for $N \sim 4P$, the holes stopped at 7 $\mu$m after 200 min. The striking difference between bilayer and blend samples is an indication that the mechanism of film stabilization is quite different when the brush is already formed, compared to the case when the brush formation takes place during the hole growth. In the former case, when a pure matrix polymer film is deposited on top of the adsorbed copolymer layer, a distinct interface between the polymer layers is created, resulting in autophobic behavior. On the other hand, in the case of blends, the copolymer adsorbs to the substrate during dewetting, resulting in a brush with a low grafting density and broad interface. The degree of entanglements between the dangling PS block and the matrix chains is expected to play an important role in viscous dissipation during slippage as discussed later.

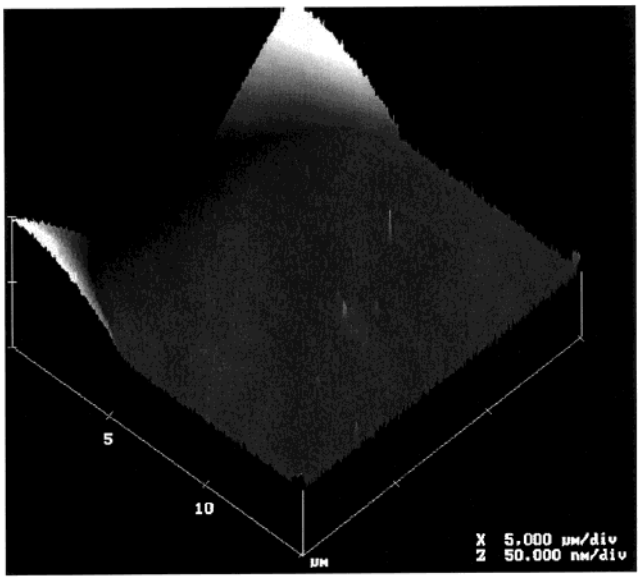


**Figure 6.** AFM micrograph of the hole floor for the pure PS film (822 Å) after 60 min at 175 °C. The features in the center mark the nucleation site. Overall, the hole floor is smooth. The smooth rim (white) has a contact angle of 2.6°.

**3.4. The Hole Floor Morphology.** To complement the hole growth studies, AFM was used to investigate the morphology of the hole floor inside the rim for selected films, namely pure PS and the PS:PS-*b*-PMMA blend ($N \sim P$). Holes with similar diameter, ca. 15 $\mu$m, were chosen for comparison. Figure 6 shows part of the inside rim wall (white) and hole floor (gray) for a PS film (822 Å) annealed at 175 °C for 60 min. The small bright patch in the middle of the hole is the nucleation site for dewetting. The contact angle between the rim and hole floor is $\sim 2.6 \pm 0.5°$, in good agreement with values reported by Leibler et al.[16] For the height scale in Figure 6, the hole floor is macroscopically smooth. To further exemplify the hole floor microroughness, a PS film was annealed to achieve complete dewetting. Between the large drops, the root-mean-square (rms) roughness is approximately 18 Å over a 10 $\mu$m $\times$ 10 $\mu$m area. This microscale roughness is much greater than the oxide roughness of about 2 Å. For the oxide layer thickness of ca. 20 Å, our results are consistent with dewetting studies of PS films by Muller-Buschbaum et al.,[39] who observed nanoscopic droplets between large drops on silicon oxide. The authors suggest that the small droplets result from nano-dewetting of a residual thin film left on the hole floor. Thus, a thin, smooth layer of PS likely covers the hole floor shown in Figure 6.

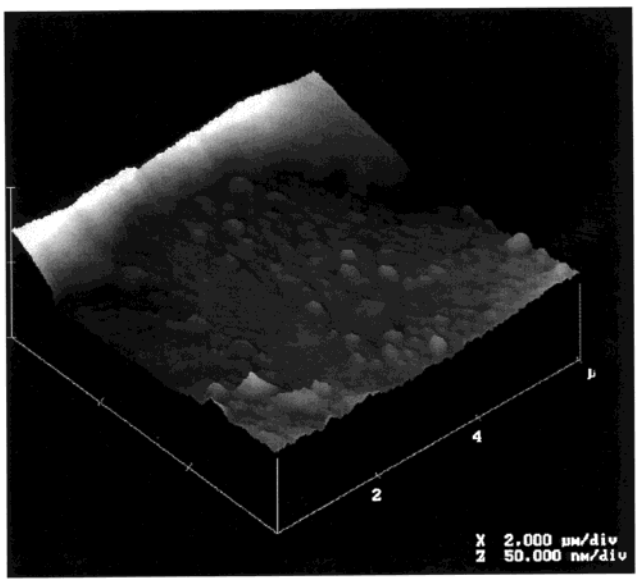


**Figure 7.** AFM micrograph of the hole floor for the blend sample of PS and PS-*b*-PMMA ($N \sim P$) (810 Å) after 600 min at 175 °C. The PS-*b*-PMMA volume fraction is 0.05. In contrast to Figure 6, the hole floor is rough with patches of polymer and the rim (white) has fingers projecting toward the center. The contact angle is about 1.3°. The area around the nucleation site is relatively smooth.

Using the same height scale, Figure 7 shows the hole floor morphology for the blend sample after 600 min at 175 °C. The isolated patch of material in the middle of the hole is the nucleation site. The most significant difference between Figures 6 and 7 is that the hole floor of the blend sample contains large patches of polymer droplets with a diameter of about 4000 Å. Note that these large droplets are absent for the pure PS film. The average patch height is about 60 Å, approximately the radius of gyration of the PS block. At present, the patch composition is unknown. The bright feature at the top-left part of the image is the rim of the hole. In contrast to the smooth interface for the pure PS sample (Figure 6), the polymer at the foot of the rim fluctuates toward the center of the hole floor. Note that one of these fluctuations is about to pinch off and form a patch. Thus, these fingers appear to produce patches as the rim retracts. Away from these rim fluctuations, the contact angle between the polymer and hole floor is ca.1.3°, which is $^1/_2$ the value for the pure PS film.

## 4. Discussion

Thin films of PS have been stabilized by the addition of a block copolymer having a short anchoring block and a long, entangling block. Thin film stability has been quantified by examining hole growth as a function of the $N$ to $P$ ratio and copolymer concentration, as well as sample geometry. Using AFM, analysis of the hole morphology reveals that the addition of copolymer decreases the rim contact angle and produces polymer patches that cover the hole floor. These studies provide a basis for understanding the mechanism of stabilization.

As holes grow, the rim velocity is determined by the difference between the capillary driving force, $F_D$, and the forces resisting hole growth. For block copolymer brushes on a substrate, these resistive forces include the energy cost to stretch and pull out adsorbed chains, $F_A$, and the viscous drag on the rim, $F_V$. Moreover, the interpenetration between the matrix and the block copolymer chains will also provide a resistive force against hole growth, $F_W$. Thus, for holes to grow, the following condition must be satisfied:

$$F_D > F_A + F_V + F_W \tag{2}$$

The driving force is given by

$$F_D \propto \gamma\theta^2 \tag{3}$$

where $\gamma$ and $\theta$ are the interfacial tension between the matrix and the adsorbed copolymer film and the dynamic contact angle, respectively.[16,22] The stretching and pull-out force is

$$F_A \propto \sigma L \tag{4}$$

where $\sigma$ and $L$ are the areal density of the adsorbed chains and the distance chains are stretched, respectively.[22] Leibler et al.[16] proposed that the resistive force originating from entanglement between matrix and copolymer chains is

$$F_W \propto -1/w \tag{5}$$

where $w$ is the interfacial width. Note that the adsorbed layer is presumed to uniformly coat the substrate. Depth profiling studies and calculations of the critical micelle concentration suggest that the PS-*b*-PMMA forms a contiguous layer on the substrate.[35]

Using eq 2, we can begin to interpret the hole growth results for the three different systems, namely, films of homopolymer, blend, and bilayer. To explain why film stability differs for these systems, the unique forces involved in each particular case are discussed. First, we compare homopolymer dewetting with blends of homopolymer and PS-*b*-PMMA additive. Using neutron reflectivity and forward recoil spectrometry, dPS-*b*-MMA in a PS film was shown to strongly segregate to the oxide interface.[34,36] Upon adsorption, the interfacial tension is expected to decrease and, consequently, the driving force for dewetting will be lower. Indeed, AFM experiments (see section 3.4) show that the blend has a smaller contact angle than the homopolymer film. As shown by eq 3, a small decrease in contact angle can have a large effect on the capillary driving force. In addition, the viscous drag exerted by the extended PS tails from the adsorbed block copolymer should further decrease the rate of hole growth. As pointed out for end-grafted polymers, $F_A$ will provide resistance against hole growth. Figure 7 shows that patches cover the hole floor for a blend film, suggesting that viscous frictional forces, $F_V$, play an important role at the PS/$SiO_x$ interface. To determine whether PS-*b*-PMMA is found throughout or under the patch, techniques providing excellent lateral resolution, such as near edge X-ray adsorption fine structure microscopy, will be needed. In summary, upon the addition of block copolymer to thin films, hole growth slows down because the driving force is reduced and resistive forces, particularly $F_A$ and $F_V$, are produced.

In previous studies (cf. Introduction), dewetting experiments focused on films prepared by applying a brush directly to the substrate followed by deposition of a homopolymer layer. Although one study[30] had compared blends and bilayers, a more quantitative

study comparing these two sample geometries is lacking. Our experiments clearly show that blending can be a more effective route to stabilize thin films. The underlying difference between bilayers and blends is the degree of interpenetration between the adsorbed copolymer and the matrix chains. In the bilayer case, the interface is narrow, and therefore $F_W$ and $F_V$ are large and small, respectively. The narrow interface between the matrix polymer and its grafted compliment is responsible for autophobic behavior.[16−18] On the other hand, the broad interface in the blend system leads to high resistive forces against dewetting, which results in film stabilization.

For the blend studies, PS-*b*-MMA molecular weights were chosen such that the PS block length was similar to the matrix length, $N \sim P$, or much longer than the matrix length, $N \sim 4P$. Figure 2 shows that hole growth is slower for the $N \sim 4P$ case. In previous studies[36] we found that the interfacial width between the brush and the polymer matrix decreases rapidly with increasing $P$ and then becomes constant for $P > 2N$. Thus, the PS-*b*-MMA with the longer PS block will penetrate more deeply into the matrix polymer than the copolymer with a short block. Therefore, the resisting force due to $F_W$ (and $F_V$) will be more effective for the $N \sim 4P$ case, as demonstrated in Figure 2.

As shown in Figure 4, the hole growth velocity decreases as the volume fraction of PS-*b*-MMA increases for the blend having $N \sim P$. As the bulk volume fraction of PS-*b*-MMA increases, the area density of adsorbed copolymer will increase until a balance is achieved between chain stretching driven by excluded volume and the associated entropy cost. Thus, $F_A$ appears to be the dominant resisting force underlying the behavior shown in Figure 4.

To completely describe blends, new theories are needed to account for both the kinetics of brush formation and the driving forces underlying dewetting. Current theories[16,25−27] assume an "equilibrium" polymer brush and are therefore more applicable to the bilayer system. A further challenge will be to incorporate the energy cost to pull out brushes from the substrate. This mechanism for energy dissipation, which likely takes place in our system, can greatly slow down hole growth. In addition to interpreting our experiments, a hybrid thermodynamic/dynamic model can provide a fundamental understanding of commercial coatings, which contain multiple components.

## 5. Conclusion

The goal of this study is to provide guidelines for using block copolymer additives to stabilize films. Using optical and atomic force microscopies, we have investigated the dewetting behavior of thin PS films with PS-*b*-PMMA additives from $SiO_x$. By blending PS-*b*-PMMA with PS, hole growth is dramatically slower than the pure PS film. Moreover, the addition of PS-*b*-PMMA prevents hole coalescence over the lifetime of the experiments, in contrast with the behavior of PS films, where holes rapidly break up to form droplet patterns. In agreement with predictions,[25−27,40] a high molar mass brush ($N \sim 4P$) stabilizes films more effectively than a brush with a lower molar mass ($N \sim P$), consistent with the greater matrix chain penetration in the former case. The optimal copolymer concentration is found to be about 3 vol %, beyond which no significant improvement in film stability is observed.

In addition, we observe significantly different dewetting behavior for bilayer and blend samples. Although slower than the pure PS case, hole growth in bilayers is faster than in films containing a blend. Moreover, holes in bilayer samples continue to grow, until they coalesce, and form droplets, indicative of autophobic behavior. The film stabilizing effect of block copolymers can be attributed to the decrease in capillary driving force, the degree of entanglements at the matrix/copolymer interface, and the brush grafting density on the substrate.

**Acknowledgement:** This work was supported by NSFOMR96-32598 and INT94-17523 and U.S.−Czech. Sci. and Tech. Program, 95009 and PRF 34081-AC7.

## References and Notes

(1) Brochard-Wyart, F.; Daillant, J. *Can. J. Phys.* **1990**, *68*, 1084.
(2) Redon, C.; Brochard-Wyart, F.; Rondelez, F. *Phys. Rev. Lett.* **1991**, *66*, 715.
(3) Vrij, A. *Discuss. Faraday Soc.* **1967**, *42*, 23. Ruckenstein, E.; Jain, R. K. *J. Chem. Soc., Faraday Trans. 2.* **1974**, *70*, 132. Williams, M. B.; Davis, S. H. *J. Colloid Interface Sci.* **1982**, *90*, 220.
(4) Khanna, R.; Sharma, A. *J. Colloid Interface Sci.* **1997**, *195*, 42.
(5) deGennes, P. G. *Rev. Mod. Phys.* **1985**, *57*, 827.
(6) Brochard-Wyart, F.; deGennes, P. G. *Adv. Colloid Interface Sci.* **1992**, *39*, 1.
(7) Brochard-Wyart, F.; deGennes, P. G.; Hervert, H.; Redon, C. *Langmuir* **1994**, *10*, 1566.
(8) Brochard-Wyart, F.; Debregeas, G.; Fondecave, R.; Martin, P. *Macromolecules* **1997**, *30*, 1211.
(9) Reiter, G. *Phys. Rev. Lett.* **1992,** *68*, 75.
(10) Reiter, G. *Langmuir* **1993**, *9*, 1344.
(11) Sharma, A.; Reiter, G. *J. Colloid Interface Sci.* **1996**, *178*, 383.
(12) Shull, K. R.; Karis, T. E. *Langmuir* **1994**, *10*, 334.
(13) Zhao, W.; Rafailovich, M. H.; Sokolov, J.; Fetters, L. J.; Plano, R.; Sanyal, M. K.; Sinha, S. K.; Sauer, B. B. *Phys. Rev. Lett.* **1993**, *70*, 1453.
(14) Feng, Y.; Karim, A.; Weiss, R. A.; Douglas, J. F.; Han, C. C. *Macromolecules* **1998**, *31*, 484.
(15) deGennes, P. G. *Macromolecules* **1980**, *13*, 1069.
(16) Leibler, L.; Ajdari, A.; Mourran, A.; Coulon, G.; Chatenay, D. In *Ordering in Macromolecular Systems*; Teramoto, A., Kobayashi, M., Norisuje, T., Eds.; Springer-Verlag: Berlin, 1994; pp 301−311.
(17) Shull, K. R. *Faraday Discuss.* **1994**, *98*, 203.
(18) Shull, K. R. *Macromolecules* **1996**, *29*, 8487.
(19) Hare, E. F.; Zisman, W. A. *J. Phys. Chem.* **1955**, *59*, 335.
(20) Liu, Y.; Rafailovich, M. H.; Sokolov, J.; Schwarz, S. A.; Zhong, X.; Eisenberg, A.; Kramer, E. J.; Sauer, B. B.; Satija, S. *Phys. Rev. Lett.* **1994**, *73*, 140.
(21) Reiter, G.; Auroy, P.; Auvray, L. *Macromolecules* **1996**, *29*, 2150.
(22) Reiter, G.; Schultz, J.; Auroy, P.; Auvray, L. *Europhys. Lett.* **1996**, *33*, 29.
(23) Henn, G.; Bucknall, D. G.; Stamm, M.; Vanhoorne, P.; Jérôme, R. *Macromolecules* **1996**, *29*, 4305.
(24) Kerle, T.; Yerushalmi-Rozen, R.; Klein, J. *Macromolecules* **1998**, *31*, 422.
(25) Martin, J. I.; Wang, Z.-G.; Schick, M. *Langmuir* **1996**, *12*, 4950.
(26) Brochard-Wyart, F.; Gay, C.; deGennes, P. G. *Macromolecules* **1996**, *29*, 377.
(27) Long, D.; Ajdari, A.; Leibler, L. *Langmuir* **1996**, *12*, 1675.
(28) Yerushalmi-Rozen, R.; Klein, J.; Fetters, L. J. *Science* **1994**, *263*, 793.
(29) Yerushalmi-Rozen, R.; Klein, J. *Phys. World* **1995**, *8*, 30.
(30) Yerushalmi-Rozen, R.; Klein, J. *J. Phys.: Condens. Matter* **1997**, *9*, 7753.
(31) Reiter, G.; Sharma, A.; Casoli, A.; David, M.; Khanna, R.; Auroy, P. *Langmuir* **1999**, *15*, 2551.
(32) Yuan, C.; Ouyang, M.; Koberstein, J. *Macromolecules* **1999**, *32*, 2329.
(33) Vlcek, P. Department of Anionic Polymerization, Institute of Macromolecular Chemistry, Czech Academy of Sciences, Prague, Czech Republic.

(34) Kobayashi, K.; Sugimoto, S.; Yajima, H.; Araki, K.; Imamura, Y.; Endo, R. *Bull. Chem. Soc. Jpn.* **1990**, *63*, 2018.
(35) Oslanec, R. Ph.D. Thesis, University of Pennsylvania, Philadelphia, PA, 1997.
(36) Oslanec, R.; Vlcek, P.; Hamilton, W. A.; Composto, R. J. *Phys. Rev. E* **1997**, *56*, 2383.
(37) Oslanec, R.; Composto, R. J.; Vlcek, P. *Macromolecules* **2000**, *33*, 2200.
(38) Faldi, A.; Composto, R. J.; Winey, K. *Langmuir* **1995**, *11*, 4855.
(39) Muller-Buschbaum, P.; Van Hoorne, P.; Scheumann, V.; Stamm, M. *Europhys. Lett.* **1997**, *40*, 655.
(40) Ferreira, P.; Adjari, A.; Leibler, L. *Macromolecules* **1998**, *31*, 3994.

MA9919312